Egypt. J. Chem. **Vol. 67**, No. 4 pp. 309 - 313 (2024)

Egyptian Journal of Chemistry

http://ejchem.journals.ekb.eg/

Highly Conductive N-type Aluminum Dopped Zinc Oxide for CZTS Kieserite Solar Cell

Enas Ahmed[1], Moshera Samy[2], and Laila Saad[1]

[1]*Department of Renewable Energy Science and Engineering, Faculty of Postgraduate Studies for Advanced Sciences, Beni-Suef University, Beni Suef, Egypt.*

[2]*Polymers and Pigments Department, National Research Centre, Dokki, 12622, Egypt.*

Abstract

Aluminum-doped zinc oxide (ZnO) is a semiconductor material with a wide band gap energy of approximately 3.4 eV and a high binding energy of around 60 meV. These characteristics confer several advantages, including the ability to withstand high breakdown voltages and sustain large electric fields. The inclusion of aluminum also enhances the electrical conductivity of zinc oxide. In this study, we employed a hydrothermal method, using zinc acetate as the source of ZnO, to synthesize AZO nanoparticles by incorporating aluminum. We conducted a thorough examination of the structural, morphological, and electrical properties of these Al-doped ZnO nanoparticles using X-ray diffraction (XRD), scanning electron microscopy (SEM), and Hall effect measurements. Additionally, we utilized the synthesized AZO as a buffer layer in CZTS-based solar cells, with the structure [Mo/ CZTS /CdS/AZO/Au], achieving a commendable conversion efficiency of 5%.

Keywords: CZTS Kesterite; Morphology; synthesis techniques; electric chracteristics.

Introduction:

ZnO possesses elastic constants that are smaller compared to relevant III-V semiconductors. Additionally, its exceptional thermal properties, such as high heat capacity, heat conductivity, low thermal expansion, and a high melting temperature, make it highly desirable for various applications, including ceramics.[1, 2] ZnO finds utility across a diverse range of industries, such as solar cells, gas sensors, ultrasonic oscillators, photocatalyst applications, the rubber industry, the textile industry, and transistor technology. Notably, ZnO exhibits n-type characteristics, and its properties can be further enhanced through doping with cationic elements like aluminum and indium or by anionic replacement with fluorine.[3, 4]

In recent times, there has been a surge of interest in aluminum-doped ZnO (AZO) due to its exceptional attributes. AZO exhibits low resistance in acidic solutions, making it suitable for various applications.[5] Furthermore, it boasts low toxicity and is cost-effective to produce, adding to its appeal. Importantly, aluminum doping significantly improves the electrical conductivity of ZnO.[5] In polymer solar cells, AZO (aluminum-doped zinc oxide) serves as a transparent conductive electrode, facilitating light transmission to the active layer for improved electrical conduction and charge collection. Its adaptability to low-temperature processes and mechanical flexibility makes it a promising candidate for flexible and lightweight solar cell technologies, while its stability enhances overall efficiency and sustainability.[6] [7] Herein, we synthesized AZO nanoparticles through a hydrothermal process, employing zinc acetate as the source of ZnO and introducing aluminum as the dopant. Our investigation focused on comprehensively analyzing the structural, morphological, and electrical characteristics of the resulting Al-doped ZnO nanoparticles.[8] To achieve this, we employed X-ray diffraction (XRD), scanning electron microscopy (SEM), and Hall effect measurements. This research contributes valuable insights into the potential applications and performance of AZO nanoparticles in various technological fields.

Methods

Materials:

Zinc acetate dehydrate ($Zn(CH_3COO)_2.2H_2O$) as zinc precursor, Al- nitrate ($Al(NO_3)_3$), methanol as solvent and sodium hydroxide (NaOH), anhydrous cadmium Chloride ($CdCl_2$) and thiourea($CS(NH_2)_2$),

*Corresponding author E-mail: Laila.hamam@psas.bsu.edu.eg,

Receive Date: 09 October 2023, Revise Date: 14 October 2023, Accept Date: 15 October 2023

DOI: https://doi.org/10.21608/ejchem.2023.241700.8724

©2024 National Information and Documentation Center (NIDOC)

$CuCl_2.2H_2O$, $ZnCl_2$, $SnCl_2.2H_2O$, $SC(NH_2)_2$, acetic acid and Soda Lime Glass (SLG) (5 cm × 5 cm).

Synthesis of AZO

AZO (Aluminum Zinc Oxide) nanoparticles were synthesized using two distinct masses of zinc acetate as the precursor material. In the first case, 1.9 grams of zinc acetate dihydrate were solubilized in 80 milliliters of methanol at room temperature. In the second scenario, 10.9 grams of zinc acetate dihydrate were dissolved in 260 milliliters of methanol. Subsequently, 0.189 grams of aluminum nitrate were dissolved in 20 milliliters of methanol and added to the zinc acetate solution. The mixture was agitated for several hours.[2, 9]

To attain a solution with a pH in the range of 11 to 12, a 3M solution of sodium hydroxide (NaOH) was added incrementally until a white precipitate formed. The solution was left to stir continuously overnight at room temperature. The white colloid was then placed in an autoclave and heated to 200 degrees Celsius for 12 hours.

Finally, the precipitate was thoroughly washed multiple times with distilled water and dried at 100 degrees Celsius for 24 hours. Figure 1 offers a visual summary of the key stages involved in the synthesis of AZO nanoparticles.

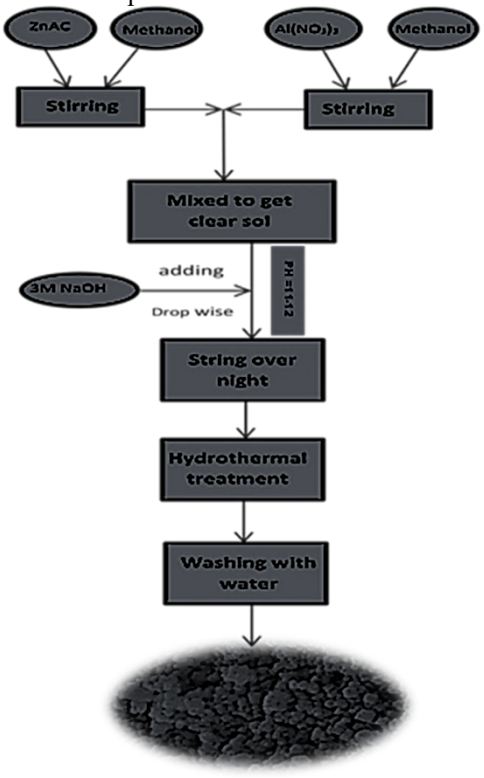

Figure 1: Schematic Representation of the Synthesis Process for AZO Nanoparticles

Device Fabrication

Deposition of kieserite layer (CZTS) Spray pyrolysis technique

$CuCl_2.2H_2O$ (0.1M), ZnCl2 (0.1M), $SnCl_2.2H_2O$ (0.1M) and $SC(NH_2)_2$ (0.8M) were added into a solvent mixture of acetic acid (20mL), distilled water(30mL) and ethanol (50mL). he solution was agitated for one hour to prevent the formation of any deposits. Upon completion of this step, a yellow solution was obtained. Glass substrates were cleansed with a 5% HNO_3 solution, followed by thorough rinsing with distilled water and ethanol.[2] Subsequently, the substrates were exposed to a temperature of 300ºC, and the CZTS solution was applied to the heated glass substrates using a spray gun powered by an air compressor (see Figure 1.a). The nozzle-to-substrate distance was maintained at 20cm. However, the initial films exhibited uneven surfaces due to the sporadic spray patches and the substantial size of the droplets from the spray gun. To rectify this issue, we replaced the spray gun with a nebulizer under the same conditions (see Figure 1.b). This adjustment resulted in the production of uniform and homogeneous thin films, possibly owing to the nebulizer's ability to disperse the solution as finely distributed fog. Subsequently, the prepared thin films were annealed at 320ºC for a duration of 12 hours.

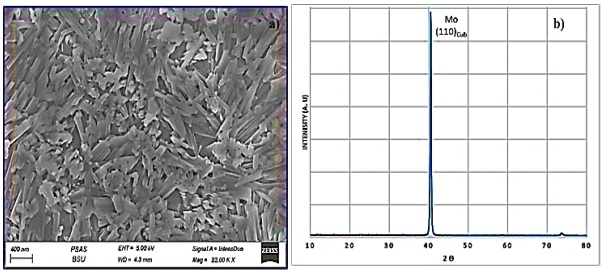

Figure 5: a) SEM morphologies and b) XRD pattern of Mo-sputtered films grown at DC power.

Molybdenum (back contact) deposition process

Molybdenum is employed as the back contact material in the CZTS-based solar cell. The fabrication process starts with the deposition of a Mo layer on the substrate.[10] In this process, Soda Lime Glass (SLG) measuring 5 cm × 5 cm is used as the substrate for growing Mo thin films via DC magnetron sputtering. Initially, the substrates are subjected to mechanical scrubbing with distilled water to remove any surface dust particles. Subsequently, they are cleaned ultrasonically using methanol for 15 minutes, followed by a similar treatment with acetone for 15 minutes and another 15-minute rinse with methanol.[10]

The target material used is Mo, and prior to the deposition of thin films, the Mo target is pre-sputtered in an argon (Ar) atmosphere for approximately 20 minutes to establish an oxide-free environment within the chamber. Before deposition, the sputtering chamber is evacuated to a base pressure of 1.5 × 10−5 Torr. Pure argon gas (99.99%) is introduced into the chamber with a flow rate of 2.0 SCCM. To achieve the desired structural and morphological properties of Mo as the back contact material for thin film solar cells, a DC power of 200 watts is applied.

Cadmium sulphide (n-type buffer layer)

The CZTS solar cell's Cadmium Sulfide (CdS) buffer layer was fabricated by employing the Chemical Bath Deposition (CBD) method. This method utilized anhydrous cadmium chloride ($CdCl_2$) and thiourea ($CS(NH_2)_2$) as sources for cadmium and sulfur ions, respectively. The study involved a systematic variation of bath temperature and thiourea concentration to determine the optimal layer thickness. An investigation was conducted to assess the influence of bath temperature, deposition time, and the [S]/[Cd] ratio within the solution on the structural, morphological, chemical composition, and optical properties of the resulting films. Films deposited under the identified optimal conditions (at a bath temperature of 80°C, a deposition time of 70 minutes, and an [S]/[Cd] ratio of 3.5) exhibited relatively well-defined crystalline structures.

CZTS-based Solar Cells assembling

CZTS solar cells were fabricated using the preprepared materials, Mo-SLG substrate was used as substrate and back-contact for the cells and the active layer CZTS.[10] To make the P-n junction buffers (n-type) CdS was deposited from chemical bath deposition.[10] AZO layer was deposited on the top of CdS layer and finally, the Au front- contact was sputtered on the top of the cell, with the structure [Mo/ CZTS /CdS/AZO/Au].

Results and Discussion

Structure and Optical properties of Al-dopped ZnO

In Figure 2, the X-ray diffraction (XRD) pattern demonstrates that the introduction of aluminum (Al) as a dopant did not result in any changes to the hexagonal wurtzite structure (JCPDS89-0510) of the ZnO nanoparticles. This suggests the formation of a single-phase compound referred to as AlxZn1-xO. Notably, the broadening of the diffraction peaks observed as a result of Al-doping indicates a reduction in nanoparticle size. Figure 1 reveals a slight shift of the ZnO nanoparticles' peak corresponding to the (101) plane toward lower angles due to the presence of Al as a dopant. This shift

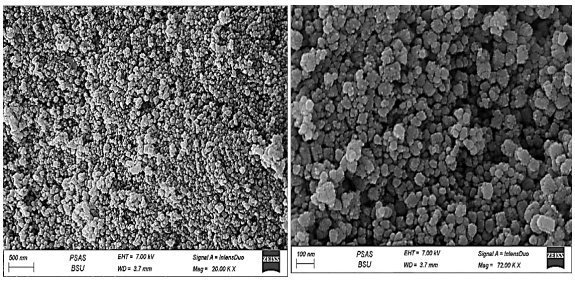

Figure 3: SEM morphologies of AZO powder with different

likely arises from the integration of dopant ions into the host material's lattice, an effect previously documented by other researchers.[11, 12]

Crystallite size (D) for both the pure and Al-doped ZnO nanoparticles was calculated using Scherrer's formula (equation 1), where β represents the full width at half maximum (FWHM) of a peak, and λ is the wavelength of the incident X-rays. Specifically, the crystallite size for both samples was determined with reference to the most intense peak (101). The crystallite size was found to be 41 nanometers for pure ZnO nanoparticles and 39 nanometers for the Al-doped ZnO nanoparticles.[12, 13]

$$D = \frac{0.9\lambda}{\beta\cos\theta}$$

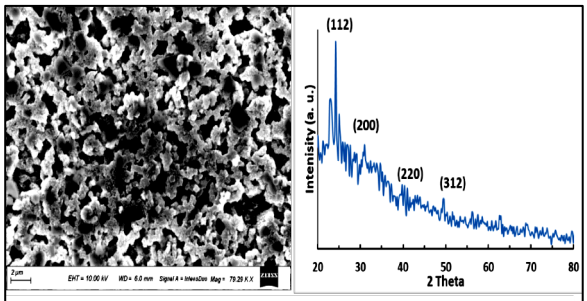

Figure 4: a) SEM morphologies and b) XRD pattern of CZTS Synthesized via spray pyrolysis

Al-dopped ZnO Morphology

The analysis of the AZO nanoparticles synthesized, as shown in Figure 3, demonstrates a uniform distribution of nanoparticles with an average size of approximately 30 nanometers. This observation is in line with the findings obtained from the X-ray Diffraction (XRD) analysis[2], as represented in Figure 2. However, for the CZTS layer prepared by spray pyrolysis technique, Figure 4, it shows a micro-channel consisted of accumulated nanoparticles where the sizes of the particles are ranged from 20 to 30 nm.

Electrical proprites of Al-dopped ZnO

The Hall effect analysis reveals the n-type conductivity of the AZO material we synthesized, as evidenced by the negative Hall

coefficient.[14, 15] Moreover, as presented in Table I, the material exhibits pronounced electrical conductivity, with a sheet resistance of 0.39 Ω per square and a resistivity measuring 2.37 × 10^-6 Ω cm.[16]

Table I the electrical parameters of the the Al-doped ZnO film.

Sample	Carriers concentration [cm^{-3}]	Conductivity [Ω^{-1} cm^{-1}]	Carrier mobility [cm^2/Vs]
AL-doped ZnO	4.4791 x 10^{23}	4.22 x 10^5	5.8577
CZTS	2.5987 x 10^{20}	7.6037 x 10^4	1.826 x 10^3

Structural Characteristics of the Mo (back contact)

The surface morphology of the Mo-sputtered film was investigated via SEM, Figure 4, shows that the substrate is fully covered with a uniform flaks-shaped molybdenum layer with no pin holes which is undesired to avoid the occurrence of short-circuit conditions after the cell fabrication. It was found that the crystallites of Mo-films have a cubic crystal structure (Figure 5). and the films possess single peak at 2θ = 40.5° with an orientation along (110) direction.

I-V measurements

The assembled cells underwent characterization through current-voltage (I-V) measurements both in the absence of light (dark) and under illumination with an AM 1.5 spectrum using a Xenon lamp to simulate solar conditions. The results of the tested cell parameters are presented in Figure 6.

Conclusion

In summary, aluminum-doped zinc oxide (AZO) emerges as a highly promising semiconductor material owing to its substantial wide band gap energy of approximately 3.4 eV and a notably high binding energy of around 60 meV. These inherent characteristics bestow upon AZO numerous advantages, such as its capability to withstand high breakdown voltages and support significant electric fields. Furthermore, the introduction of aluminum greatly augments the electrical conductivity of zinc oxide. In our research, we employed a hydrothermal synthesis method, utilizing zinc acetate as the precursor for ZnO, to successfully fabricate AZO nanoparticles through aluminum doping. We conducted a comprehensive investigation into the structural, morphological, and electrical attributes of these Al-doped ZnO nanoparticles using techniques like X-ray diffraction (XRD), scanning electron microscopy (SEM), and Hall effect measurements. Additionally, we harnessed the synthesized AZO as a buffer layer in CZTS-based solar cells, employing a layered configuration of [Mo/ CZTS /CdS/AZO/Au], resulting in an impressive conversion efficiency of 5%. The exceptional transparent conductivity, adaptability, and stability of AZO (aluminum-doped zinc oxide) render it an auspicious option for optimizing both thin-film and polymer solar cell technologies. This study underscores the potential of AZO in enhancing the performance of emerging solar cell technologies and contributes valuable insights to the field of semiconductor materials and photovoltaic devices.

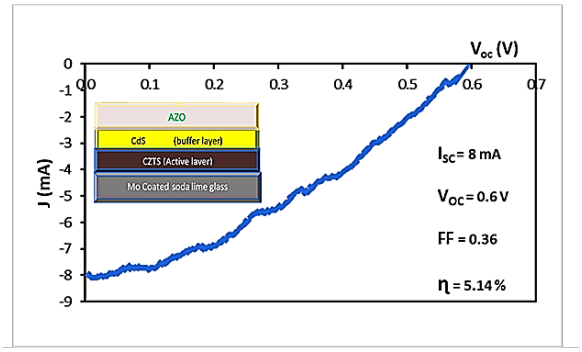

Figure 6: J-V measurements of CZTS based solar cell with structure Mo/CZTS/CdS/AZO/Au

Acknowledgement

This paper is based upon work supported by Science, Technology & Innovation Funding Authority (STDF) under grant of Call 9 / Young Researchers Grant (STDF-YRG), Project (ID 33421).

References

1. Z. Fan and J. G. Lu, Journal of Nanoscience and Nanotechnology **5** (10), 1561-1573 (2005).
2. A. V. Moholkar, S. S. Shinde, A. R. Babar, K.-U. Sim, H. K. Lee, K. Y. Rajpure, P. S. Patil, C. H. Bhosale and J. H. Kim, Journal of Alloys and Compounds **509** (27), 7439-7446 (2011).
3. A. Kołodziejczak-Radzimska and T. Jesionowski, Materials **7** (4), 2833-2881 (2014).
4. A. H. Ibrahim, L. Saad, A. A. Said, M. Soliman and S. Ebrahim, AIP Advances **12** (1) (2022).
5. J. L. Gomez and O. Tigli, Journal of Materials Science **48** (2), 612-624 (2013).
6. G. Magdy, M. E. Harb, A. M. Elshaer, L. Saad, S. Ebrahim and M. Soliman, JOM **71** (6), 1944-1951 (2019).
7. J. Jang, J.-H. Kim, S. Lee, C.-M. Oh, I.-W. Hwang, S. Kim, A. Park, D. Kang, C. Jang, T. Ki, H. Kim and K. Lee, ACS Applied Energy Materials **6** (18), 9778-9787 (2023).
8. A. Becheri, M. Dürr, P. Lo Nostro and P. Baglioni, Journal of Nanoparticle Research **10** (4), 679-689 (2008).

9. S. Sruthi, J. Ashtami and P. V. Mohanan, Materials Today Chemistry **10**, 175-186 (2018).
10. Y.-Z. Chen, S.-W. Wang, C.-C. Yang, C.-H. Chung, Y.-C. Wang, S.-W. Huang Chen, C.-W. Chen, T.-Y. Su, H.-N. Lin, H.-C. Kuo and Y.-L. Chueh, Nanoscale **11** (21), 10410-10419 (2019).
11. F. Ruske, M. Roczen, K. Lee, M. Wimmer, S. Gall, J. Hüpkes, D. Hrunski and B. Rech, Journal of Applied Physics **107** (1) (2010).
12. P. P. Sahay and R. K. Nath, Sensors and Actuators B: Chemical **133** (1), 222-227 (2008).
13. K. C. Park, D. Y. Ma and K. H. Kim, Thin Solid Films **305** (1), 201-209 (1997).
14. C. H. Liu, W. C. Yiu, F. C. K. Au, J. X. Ding, C. S. Lee and S. T. Lee, Applied Physics Letters **83** (15), 3168-3170 (2003).
15. T. Minami, Semiconductor Science and Technology **20** (4), S35 (2005).
16. J. Jie, G. Wang, X. Han, Q. Yu, Y. Liao, G. Li and J. G. Hou, Chemical Physics Letters **387** (4), 466-470 (2004).